IPTC
International Petroleum Technology Conference
Innovation and Efficiency Excellence for our Energy Future
14 - 16 November 2016
BANGKOK, THAILAND
Bangkok Convention Centre at CentralWorld

(invited)
The DC Response Of Electrically Conducting Fractures Excited By A Grounded Current Source

Chester J Weiss[1], David F Aldridge[1], Hunter A Knox[1], Kimberly A Schramm[1] and Lewis C Bartel[2]

[1]*Sandia National Laboratories* [2]*CARBO Ceramics Inc.*

Problem Statement and Approach

- Given an induced fracture system in a horizontal well with elevated electrical conductivity, what can be said about the fractures from surface measurements of DC potential differences?
- Forward model the Earth/borehole/fracture system with unstructured finite elements conformal to conductivity boundaries
  - compute the prefrack, postfrack and pre-post DC potential differences
  - parametric analysis of fracture conductivity effect
  - quantify topographic effects
  - linear inversion synthetic responses for simple fracture mapping

Finite element forward solver: Benchmark test

Solve for electric scalar potential Φ over an arbitrary conductivity model σ excited by a source current $\mathbf{J}_s$:

$$-\nabla \cdot (\sigma \nabla \Phi) = \nabla \cdot \mathbf{J}_s$$

Homogeneous Dirichlet BC on mesh bottom and sides, Neumann BC on mesh top to simulate air/Earth interface.

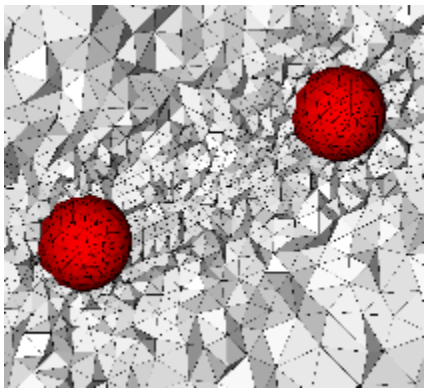

(right) *finite element mesh for benchmark comparison against analytic solution of 2 spheres in a wholespace (Aldridge and Oldenburg, Geophysical Prospecting, 1989)*

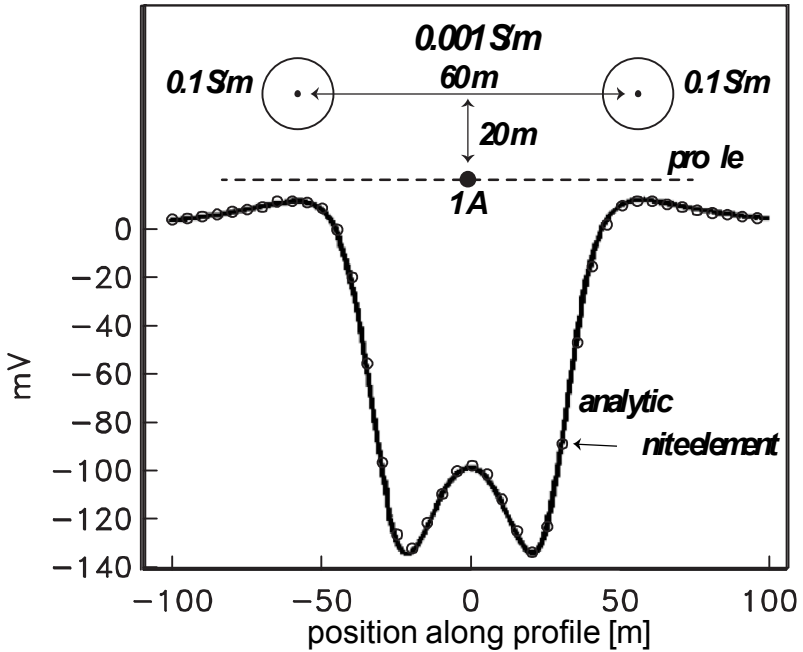

(above) *comparison of finite element and analytic solutions of scattered electric potential for an offset point source*

Earth model of exploration scenario

*Idealized **(below)** and discretized **(right)** Earth model for finite element analysis (FEA). Electrode location indicated by symbols, with 3 possible contact points (A-C) of the +'ve electrode with steel well casing.*

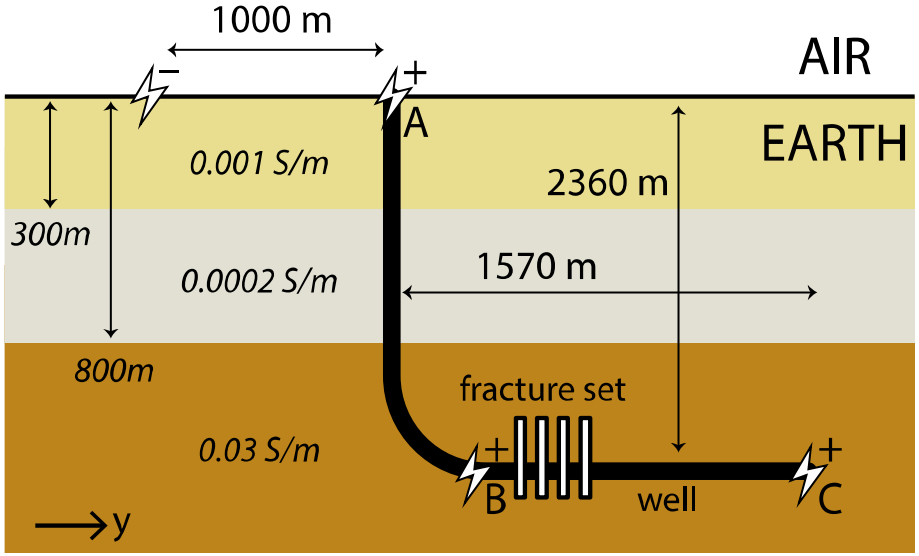

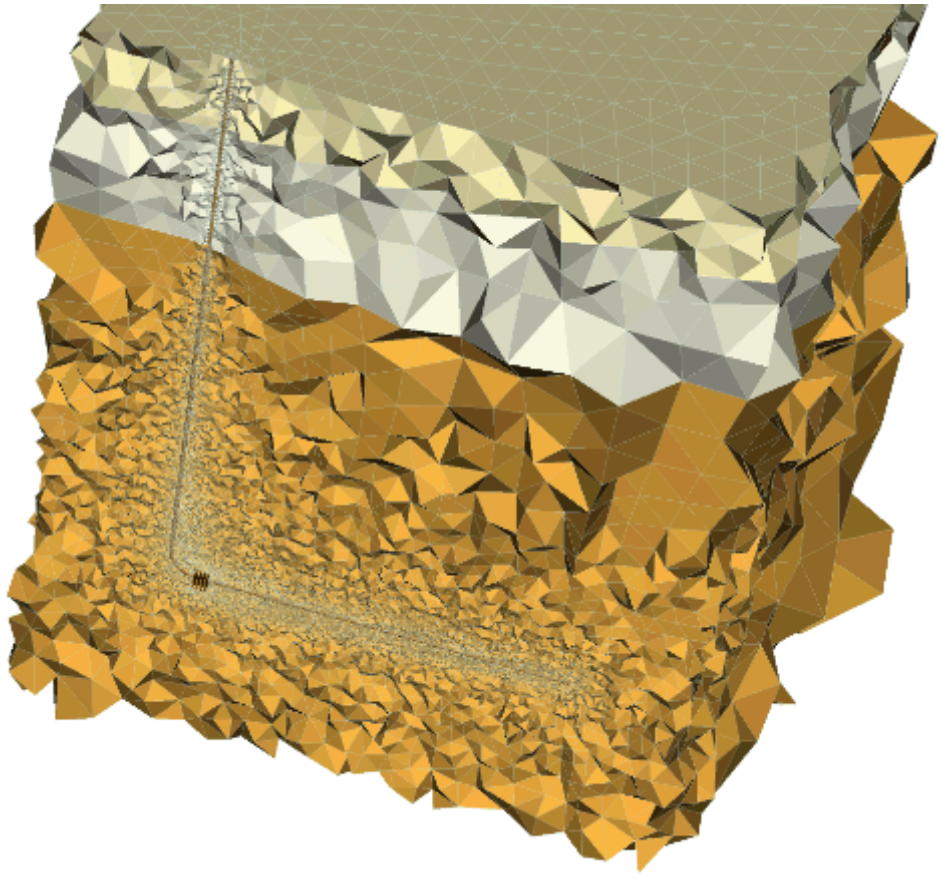

DC potential on the ground over the well head

(left) Plan view of electric potential (in Volts) at Earth's surface (z = 0 m) over the well head (x = y = 0 m) where the Earth model is energized by +1 A current source at the well head (case A) and a –1 A sink at y = 1000 m.

(right) Potential difference (in microvolts) at z = 0 m computed by subtracting the response of the Earth model with a set of 10 S/m fractures from one where the fractures are absent, thus simulating a time-lapse scenario for detection of electrically enhanced fractures.

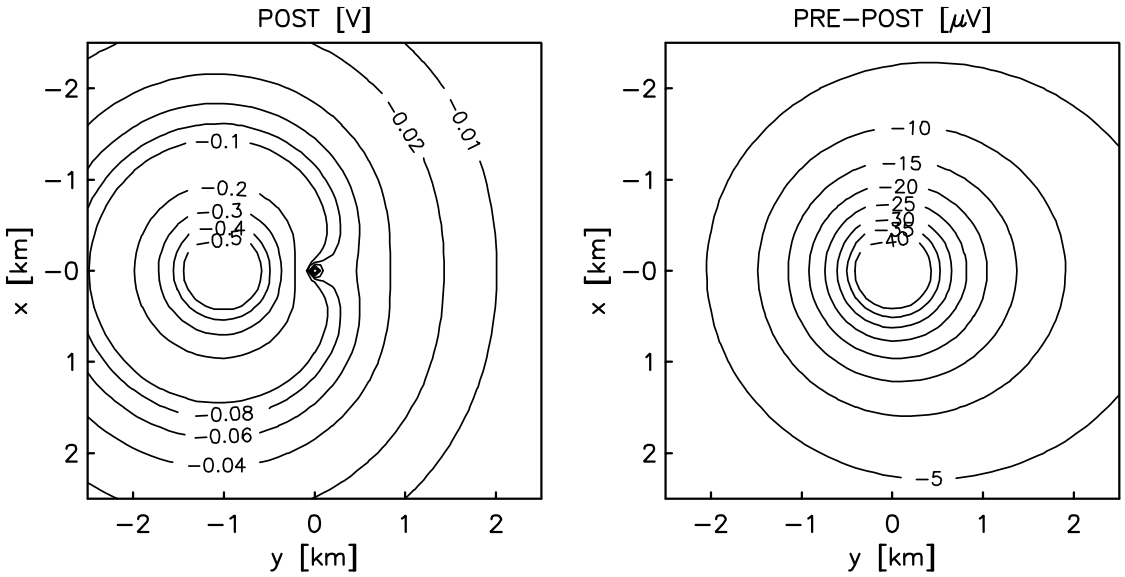

How do the ground-based measurements arise?

Oblique view of the magnitude of electric potential for case A (+'ve electrode at the well head) along two intersecting surfaces: a vertical slice at x = 0 m through the well track and fracture set; and, a horizontal slice at z = 0 m along the air/Earth interface.

Intersecting the slices are the well track and fractures. Note the local perturbation near the well heel due to the fractures, as well as the dominance of the –1 A current source on the potentials at z = 0.

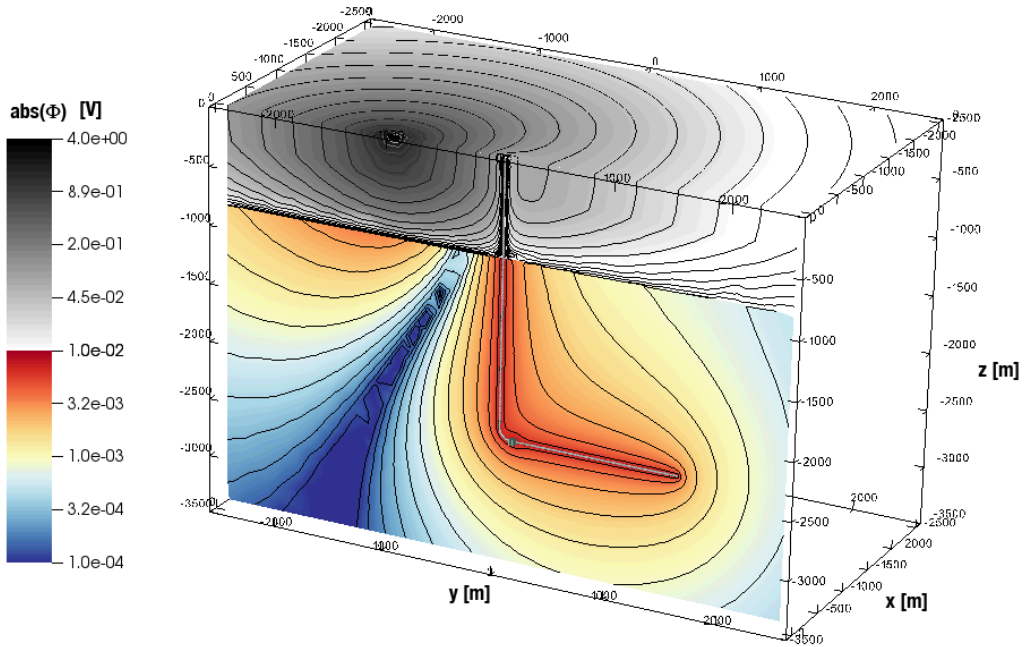

Generally small amplitudes of the potential in the region below z = −800 m are consistent with its relatively high 0.03 S/m conductivity – in contrast to the low (< 0.001 S/m) conductivity in the region above z = −800 m.

Topography effect: 3D-1D residual

Topography: 860m to 970m elevation

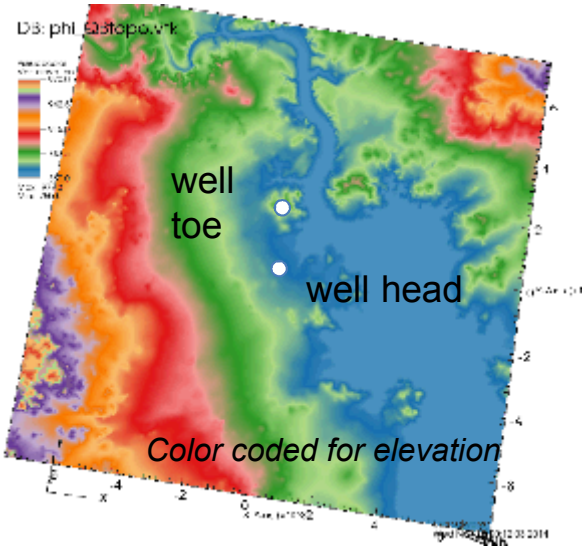

3D DC FEA calculation w/ topo

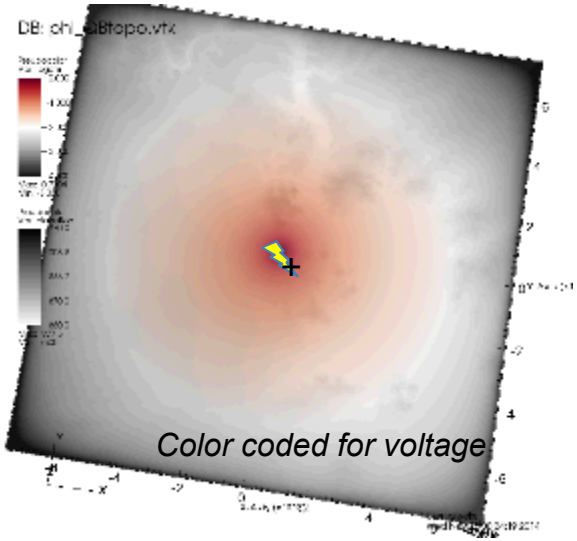

topo – flat FEA residual

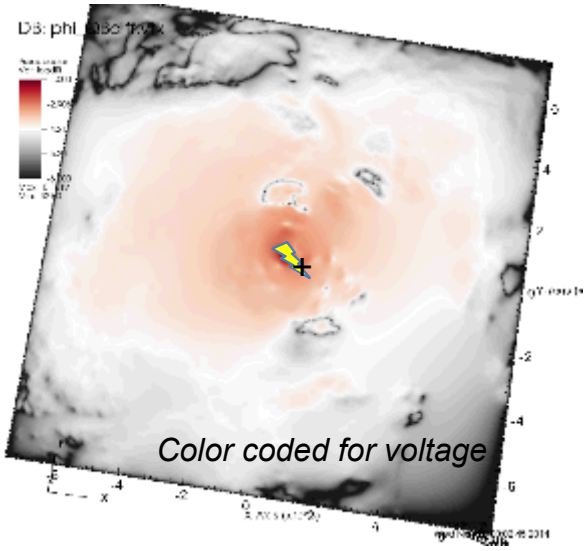

~1% change in voltage due to topography

This relative magnitude is comparable to the change expected from electrically conductive fracture set.

Predicted data for inline measurement array

(top curve) Potential difference along line x = 0 directly through the well head and over the horizontal section of the well, in the absence of conducting fractures for 1 A source located at the well head (case A) and –1 A source at y = −1000 m. Dashed lines indicate negative values; solid lines, positive.

(bottom curve) Scattered potential differences arising from a 10 S/m fracture set near the heel of the well bore.

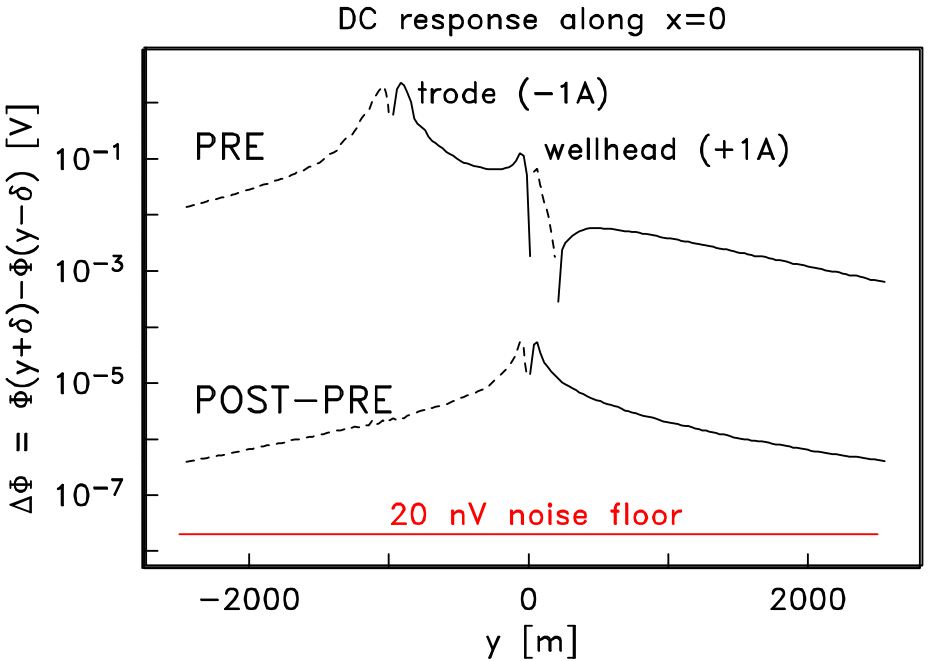

Potential differences computed using 100 m electrode separation, δ = 50 m. For reference, also shown is the 20 nV noise floor for the 32-bit ZEN receiver from Zonge Engineering (http://zonge.com/instruments-home/systems/distributed-em-systems/).

Effect of source location and fracture conductivity

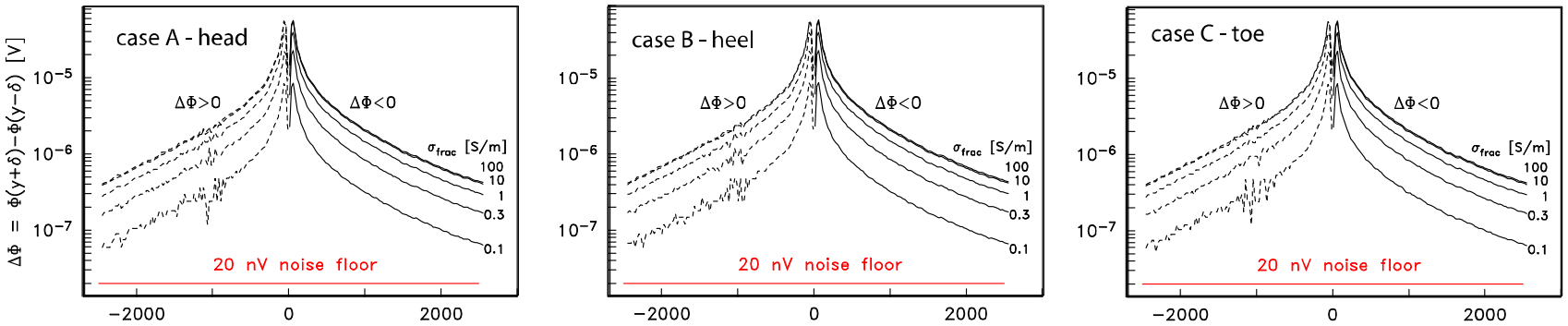

Inline scattered potential differences (δ = 50 m) as a function of fracture conductivity over the range 0.1–100 S/m for a –1 A source at y = −1000 m and +1 A source located at either the well head, heel, or toe (cases A-C). Dashed lines indicate negative values; solid lines, positive.

Note that location of the +1 A source has minimal effect on scattered potential differences, and that fracture response is saturated for conductivities greater than ~10 S/m.

Effect of fracture location

heel fracture

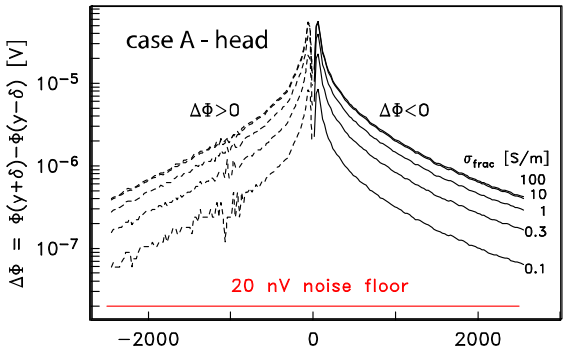

toe fracture

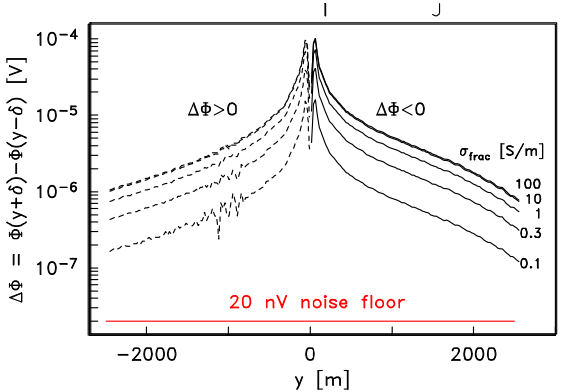

Inline scattered potential differences (δ = 50 m) as a function of fracture conductivity over the range 0.1–100 S/m for a –1 A source at y = −1000 m and +1 A source, fractures located at either the well heel **(left)**, or toe **(right)**. Dashed lines indicate negative values; solid lines, positive.

Note the pronounced left/right asymmetry of the toe-fracture result, and that fracture response remains saturated for conductivities greater than ~10 S/m.

Motivation for empirical LQS inversion

Oblique view of the magnitude of POST–PRE scattered electric potential for case A along two intersecting surfaces: a vertical slice through the well track and fracture set at x = 0 m; and, a horizontal slice along the air/Earth interface
z = 0 m.

Region where Φ > 0 is denoted by (+) whereas the region Φ < 0 is denoted by (−). Superimposed on the slices are the well bore and fractures.

Observe that this POST–PRE difference data arises primarily from a combination of sources – one due to the conductivity perturbation at the fractures, and the other, a change in the relative potential of the borehole casing due to current leakage at the fracture.

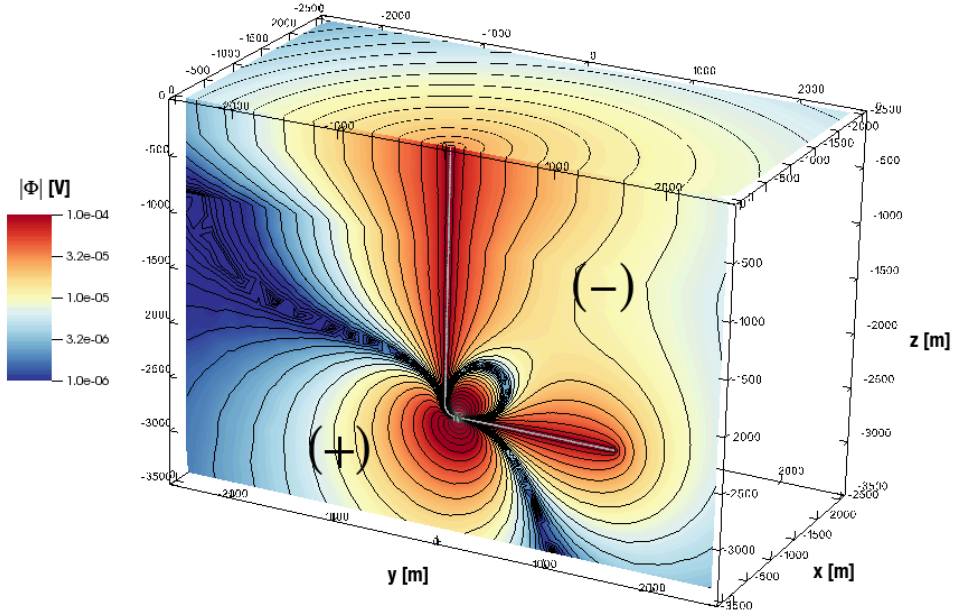

Empirical LQS inversion: invert time-lapse surface data for linear charge density (**l**ambda) on the well casing; point charge **q** at the fracture, and position **s** of the fracture.

LQS inversion: eyeball minimization of the misfit norm

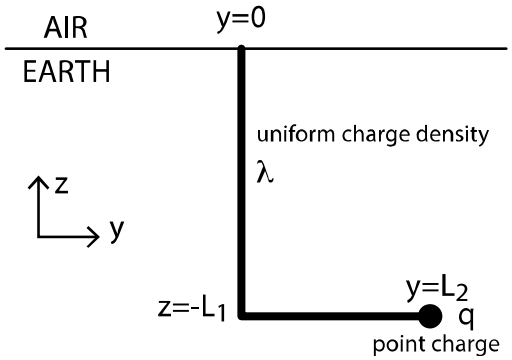

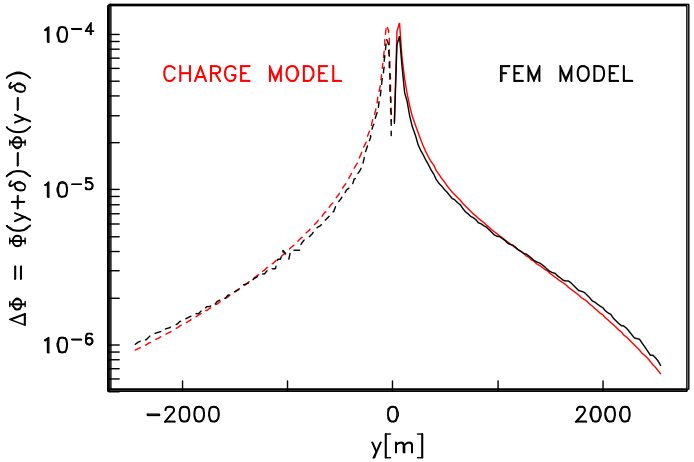

(left) problem setup for LQS inversion of toe-fracture data with known fracture location, s. Inversion is linear in charge magnitudes λ and q.

(right) eyeball-minimized data misfit of time lapse inline potential differences. λ = 5.6E-15 C/m, q = 1.7E-11 C.

LQS Inversion: minimize the L2 norm

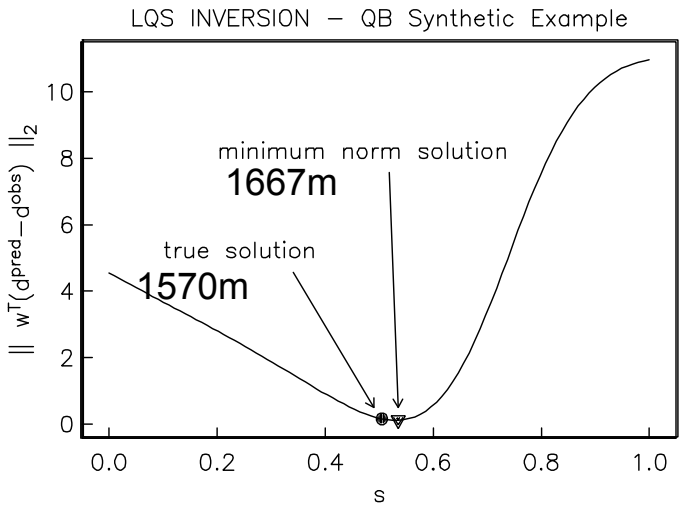

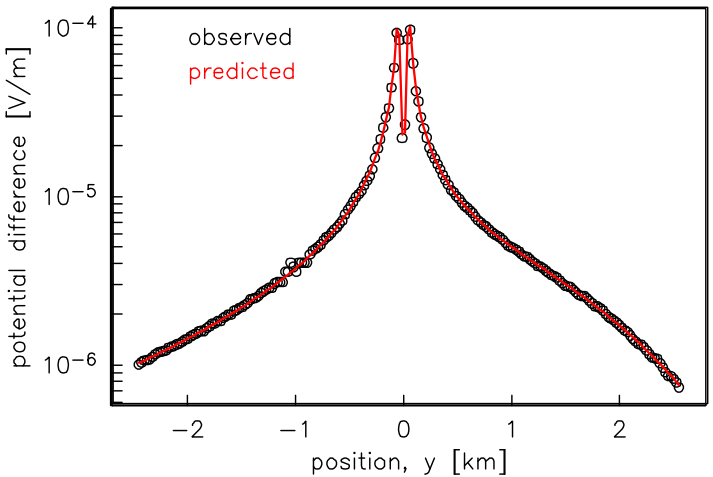

(left) Line search on s for minimum L2 misfit. At each candidate location, s, the linear inverse problem for (λ,q) is solved.

(right) L2-minimized data misfit of time lapse inline potential differences. λ = 5.1E-15 C/m, q = 1.8E-11 C.

LQS inversion: 2D array of 2-component data

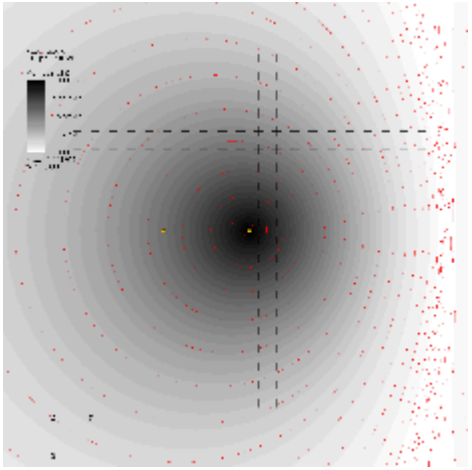

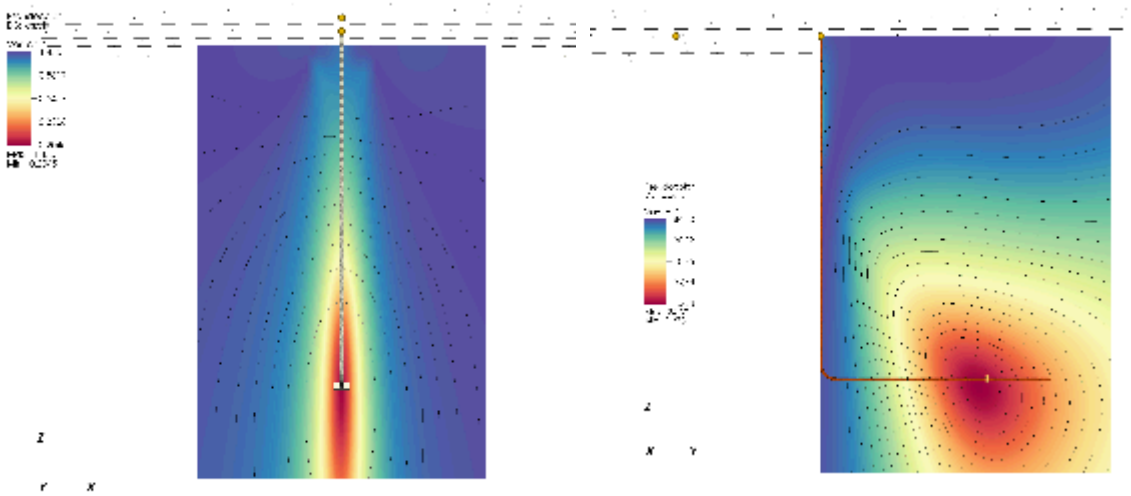

(above) Broaden the array to a *massive* 20x20 grid of 2-component measurements on a 4x4 km area. Time-lapse potentials in grey scale with red contours. Stations indicated by + signs. Well head and ground point indicated by yellow dots.

Color scaled L2 norm values of optimal (λ,q) pairs for candidate 's' points in a plane orthogonal to the horizontal section of the well bore and through the fracture set **(left)**, and in a plane containing the entire well bore **(right)**.

LQS Inversion: 3D fracture location

Inversion of synthetic data taken from a *massive* 20x20 grid of 2-component measurements on a 4x4 km area. Time-lapse potentials in grey scale with red contours.

Stations indicated by + signs. Well head and ground point indicated by yellow dots.

Red isosurface surrounding the fractures is taken at χ^2=2, a value where its width is similar to that of the fractures.

$$\chi^2 = \sum_{i=1}^{N} \left(\frac{d_i^{obs} - d_i^{pred}}{d_i^{obs}} \right)^2$$

Note the strong differences in vertical and lateral resolution!

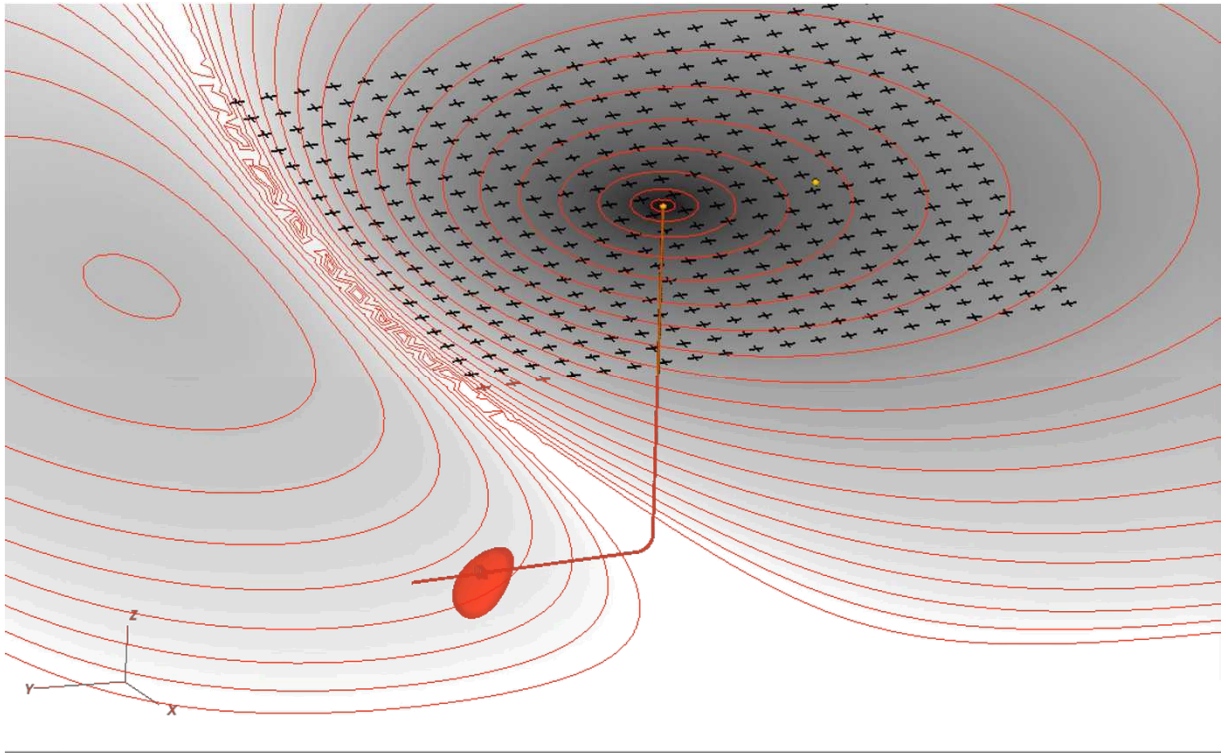

Conclusions

- Assuming electrical continuity of the well casing, DC fracture response is generally independent of source contact point.
- DC response of the fracture set saturates for conductivities greater than 10 S/m in the scenarios tested here. Further investigation is required to quantify such thresholds in other geologic settings.
- Topographic effects introduce signals comparable in magnitude to those of the fractures.
- Time-lapse DC response of the fractures is reasonably approximated by a simple 3-parameter charge model and easily invertible.

Acknowledgements / Thank You / Questions

VSR6

This work is conducted under the auspices of CRADA (Cooperative Research and Development Agreement) SC11/01780.00 between **CARBO Ceramics Inc.** and **Sandia National Laboratories**.

Sandia National Laboratories is a multi-mission laboratory managed and operated by Sandia Corporation, a wholly owned subsidiary of Lockheed Martin Corporation, for the U.S. Department of Energy's National Nuclear Security Administration under contract DE-AC04-94AL85000.

Slide 17

VSR6 I recommend getting rid of this first acknowledgment statement.
Vigil, Steven R, 10/7/2016